



## The cold storage of green bananas affects the starch degradation during ripening at higher temperature



Fernanda H.G. Peroni-Okita<sup>a</sup>, Mateus B. Cardoso<sup>c</sup>, Roberta G.D. Agopian<sup>a</sup>,  
Ricardo P. Louro<sup>d</sup>, João R.O. Nascimento<sup>a,b</sup>, Eduardo Purgatto<sup>a,b</sup>, Maria I.B. Tavares<sup>e</sup>,  
Franco M. Lajolo<sup>a,b</sup>, Beatriz R. Cordenunsi<sup>a,b,\*</sup>

<sup>a</sup> University of São Paulo, Department of Food Science and Experimental Nutrition, FCF, Cidade Universitária, CEP 05508-000 São Paulo, SP, Brazil

<sup>b</sup> University of São Paulo, NAPAN, Food and Nutrition Research Center, Cidade Universitária, São Paulo, SP, Brazil

<sup>c</sup> LNLS – Laboratório Nacional de Luz Síncrotron, Caixa Postal 6192, CEP 13083-970 Campinas, SP, Brazil

<sup>d</sup> Universidade Federal do Rio de Janeiro, CCS, Instituto de Biologia, Departamento de Botânica, Laboratório de Ultraestrutura Vegetal, Cidade Universitária, Ilha do Fundão, CEP 21941-590 Rio de Janeiro, RJ, Brazil

<sup>e</sup> Universidade Federal do Rio de Janeiro, Instituto de Macromoléculas Professora Eloisa Mano, Cidade Universitária, Ilha do Fundão, CEP 21941-598 Rio de Janeiro, RJ, Brazil

### ARTICLE INFO

#### Article history:

Received 3 December 2012

Received in revised form 12 March 2013

Accepted 15 March 2013

Available online 22 March 2013

#### Keywords:

Banana  
Low temperature  
Starch  
Degradation  
Structure  
Enzymes

### ABSTRACT

The aim of this work was to investigate the starch degradation of bananas stored at low temperature (13 °C, cold-stored group) and bananas stored at 19 °C (control group) during ripening. The starch granules were isolated during different stages of banana ripening, and their structure was investigated using different techniques. The activities of  $\alpha$ -amylase and  $\beta$ -amylase associated to the starch granules were determined, and their presence was confirmed using immunolocalization assays. The increased molecular mobility likely facilitated the intake and action of  $\alpha$ -amylase on the granule surface, where it was the prevalent enzyme in bananas stored at low temperature. The 10 days of storage at low temperature also influenced the sizes and shapes of the granules, with a predominance of rounded granules and pits on the surface along with superior amylose content, the higher amounts of amylopectin A-chains and the subtle increase in the A-type allomorph content.

© 2013 Elsevier Ltd. Open access under the [Elsevier OA license](http://www.elsevier.com/locate/elsevier).

### 1. Introduction

Banana is a typical climacteric fruit, and important physico-chemical changes take place during ripening. Thus, because this fruit has a short green-life, *i.e.*, the elapsed time between harvest and the beginning of ethylene production, the manipulation of environmental conditions, mainly the atmosphere and the temperature, is used to extend the storage time.

Storage at low temperatures is a step in the cold chain, from the harvest to market, to extend the green-life of fruit. In general terms, this condition can substantially reduce the rate of many metabolic pathways that lead to fruit senescence, deterioration and decay of quality (Chauhan, Rajei, Dargupta, & Bawa, 2006). Low temperatures temporarily impair ripening by maintaining the lowest possible ethylene concentrations (Seymour, Taylor, & Tucker, 1993;

Wills, McGlasson, Graham, & Joyce, 1998), but most tropical fruits undergo physiological disorders and deterioration of quality when exposed to low temperatures. The surface pitting at temperatures lower than 10 °C is a typical symptom of chilling injury (Imahori, Takemura, & Bai, 2008; Martínez-Romero, Serrano, & Valero, 2003; Zamorano *et al.*, 1994), and in the case of bananas, although the pulp will not be affected for several days, the skin may turn dark, which negatively affects the quality.

In bananas, the symptoms of chilling injury appear to be cultivar dependent and related to the genomic group. In Brazil, the Nanicão cv., a member of the AAA group, is commercially relevant but less resistant to low temperatures than Prata, a cultivar of the AAB group (Agopian *et al.*, 2011). According to Lichtemberg, Malburg, and Hinz (2001), the B genome appears to confer cold resistance.

Green Nanicão bananas may accumulate high levels of starch (25%), which is mostly degraded during ripening, resulting in high amounts of soluble sugars in the fully ripe fruit (22%) (Peroni-Okita *et al.*, 2010). However, the low cold resistance could be a disadvantage for the long-term storage of Nanicão bananas because the fruits exposed to low temperatures for several days may accumulate a lower amount of sugars during ripening, although a marginal

\* Corresponding author at: University of São Paulo, Department of Food Science and Experimental Nutrition, FCF, Cidade Universitária, CEP 05508-000 São Paulo, SP, Brazil. Tel.: +55 11 30913656; fax: +55 11 38154410.

E-mail address: [hojak@usp.br](mailto:hojak@usp.br) (B.R. Cordenunsi).

increase in the sucrose levels was observed during storage, which is reportedly a cyroprotective effect (Agopian et al., 2011).

This lower amount of soluble sugars in cold-stored Nanicão bananas was followed by significant changes in the activities and expression of the enzymes linked to carbon partitioning and starch levels, such as  $\beta$ -amylase, starch-phosphorylases, sucrose-phosphate-synthase and sucrose-synthase (Agopian et al., 2011). Although these changes could be partially responsible for the marginal cryoprotective effect, suggesting they may contribute to cold acclimation, the net result was a decrease in fruit quality, as the end amount of soluble sugars in the ripe fruit was lower. Therefore, a better understanding on the effects of cold on the starch-to-sucrose metabolism of commercially relevant, cold sensitive bananas is important in terms of food quality. In this regard, the structural features of the starch granules, which are the substrates for soluble sugar synthesis, may have been overlooked in the previous study, as the differences in the pattern of degradation of the granules and other parameters, such as the levels of amylose and amylopectin or even the crystallinity, may provide clues about the changes occurring in banana pulp tissue during cold acclimation.

Therefore, the aims of this study were to investigate the degradation of starch in Nanicão bananas stored at low temperature at the starch granule level. The structural characteristics of the starch granules from this cultivar were investigated to determine the crystallinity and the ratio of A- to B-type starch allomorphs, the structural water content of starch granule, the chain length distribution of amylopectin, and the amylose content. Additionally, microscopy was used to study the internal and external structural features of the granules in relation to the phosphate and amylose distribution and the occurrence of the granule-attached forms of the main enzymes involved in starch degradation.

## 2. Materials and methods

### 2.1. Material

Mature green bananas, *Musa acuminata*, AAA, cv. 'Nanicão', were obtained at CEAGESP (Companhia de Entrepósitos e Armazéns Gerais do Estado de São Paulo, Brazil) immediately post-harvest. The fruits were washed with sodium hypochlorite solution (0.1%, w/v) and were separated into two groups that were stored in different chambers as follows: fruits were stored at 19 °C (control group) until fully ripe and fruits were stored at 13 °C (cold-stored group) for 15 days. Then, the cold-stored group was stored at 19 °C until fully ripe. The degree of ripening was monitored through both the CO<sub>2</sub> and ethylene levels and the results obtained were presented in the previous work (Agopian et al. (2011)). The samples were collected, peeled, sliced, frozen in liquid N<sub>2</sub> and stored at -80 °C for future analyses.

### 2.2. Isolation of starch granules

Based on the starch degradation profile, starch granules were isolated from the pulp tissue according to Soares et al. (2011) during different stages of ripening: starches were isolated from the control fruits with 1, 10, 15, 17, 21 and 22 days after harvest, and starches were isolated from the cold-stored fruits (at 13 °C) with 10, 17, 21 and 22 days after harvest.

### 2.3. Laser differential interference contrast microscopy

Starch grains suspended in water were placed on a slide and covered by a cover slip. The starches were visualized using a Confocal laser scanning microscope (CLSM, Zeiss, Jena, Turingia, Germany,

LSM 510) and the images were analyzed in a Laser Scanning Microscopes (LSM) Image Browser Program.

### 2.4. Optical microscopy

A mixture of dried starch and 50% glycerol was fixed on a glass slide, and the analyses were conducted using a Polarizing Optics microscope (Zeiss-Axioplan 2 microscope, Carl Zeiss, Göttingen, Germany) equipped with a 3CCD camera (Color Vision Camera Module, Donpisha).

### 2.5. Scanning electron microscopy (SEM)

The samples were fixed in stubs by double face tape and coated with a 10-nm-thick platinum layer in a Bal-tec MED-020 Coating System (Kettleshulme, UK). The samples were analyzed in an FEI Quanta 600 FEG Scanning Electron Microscope (FEI Company, Oregon, USA). SEM observations were performed in the secondary electron mode operating at 2 kV, 5 kV and 10 kV.

### 2.6. Amylose content

To measure the amylose content of starch, the Megazyme enzymatic method (Kit K-AMYL 04/06, Megazyme International Ireland Ltd, Wicklow, Ireland) was used, according to Peroni-Okita et al. (2010).

### 2.7. APTS Staining

The APTS staining was performed as described by Blennow et al. (2003), and Glaring, Koch, and Blennow (2006), with the following modifications. The starch granules (5 mg) were incubated in 10  $\mu$ L of freshly made APTS solution (20 mM 8-amino-1,3,6-pyrenetrisulfonic acid, Molecular Probes, Carlsbad, USA, dissolved in 15% acetic acid) and 10  $\mu$ L of 1 M sodium cyanoborohydride. The mixture was incubated at 30 °C for 18 h. The granules were washed five times with 1 mL of distilled water and suspended in 20  $\mu$ L of 50% glycerol. For microscopy, 2  $\mu$ L of the granule mixture was fixed on a glass slide. A confocal laser scanning microscope (CLSM, Zeiss, Jena, Turingia, Germany, LSM 510) was used for detection of the fluorescence signal from the stained starch grains. For APTS, a 488 nm laser line was used for excitation, and light was detected between 500 and 535 nm. For each starch granule, a stack of horizontal optical sections was obtained according to Blennow et al. (2003). The images were analyzed in a laser scanning microscopes (LSM) image browser program.

### 2.8. Amylopectin branch chain-length distribution

The starch was debranched using isoamylase of *Pseudomonas* sp. (Megazyme International Ireland Ltd., Ireland), according to the procedure described by Peroni-Okita et al. (2010). The branch chain-length distribution of amylopectin was analyzed and calculated by using a high-performance anion exchange chromatograph equipped with a pulsed amperometric detector (HPAEC-PAD, Dionex, Sunnyvale, CA, USA), as described by Peroni-Okita et al. (2010).

### 2.9. Wide-angle X-ray diffraction (WAXD)

The WAXD diagrams were recorded using a rotating-anode X-ray diffractometer (Rigaku corporation, Danvers, MA, USA) with Ni-filtered CuK $\alpha$  radiation ( $\lambda = 1.542 \text{ \AA}$ ) operating at 50 kV and 100 mA at the Brazilian Synchrotron Light Laboratory (Campinas, Brazil), according to Cardoso and Westfahl (2010). The diffraction patterns were recorded during 10 min exposures on a mar345

image plate placed at 200.0 mm from the sample and an alumina pattern was used to achieve calibration. The measurements were made on samples after the water content was adjusted by sorption at 90% relative humidity (RH) for ten days in the presence of a saturated sodium chloride solution. The samples were prepared in thin-walled (0.01 mm) glass capillary tubes (0.7 mm in diameter). The capillary was centrifuged to pack the granules at the bottom and sealed to prevent any significant change in the water content during the measurement. The WAXD profiles were obtained by radial averaging and normalized to the integrated area between  $2\theta = 5$  and  $40^\circ$ . The WAXD patterns were used to determine the crystallinity and respective amounts of A- and B-type allomorphs as described in the literature (Thys et al., 2008).

### 2.10. NMR measurements

The relaxation time was analyzed in a Maran Ultra low-field NMR spectrometer (Oxford Instruments, UK), using an 18 mm NMR tube operated at 23 MHz for the hydrogen nucleus. The pulse sequence used to obtain the data on the spin–spin relaxation time was Carr–Purcell–Meibom–Gil (CPMG) and the  $90^\circ$  pulse of 4.7  $\mu$ s was calibrated automatically by the instrument's software. The same sample was analyzed at 27 °C and 50 °C. The relaxation values and relative intensities were obtained by fitting the exponential data with the aid of the WINFIT program. The distributed exponential fits were obtained by plotting the relaxation amplitude versus relaxation time using the WINDXP software. Both WINFIT and WINDXP are commercial programs and were bundled with the low-field NMR spectrometer.

### 2.11. Extraction of the proteins associated to the starch granule surfaces and activities of $\alpha$ - and $\beta$ -amylases

The enzymes bound to the starch granules during different stages of ripening were extracted according to Peroni et al. (2008). The extracts were concentrated in Centriprep-10 and Centricon-10, according to the manufacturer's manual (Millipore Corporation, Bedford, MA 01730 USA, 2000). The *in vitro* activity was determined after the obtained extracts were incubated with a specific substrate of  $\alpha$ -amylase (BPNPG7-Ceralpha, Megazyme) and  $\beta$ -amylase (PNPG5-Betamyl, Megazyme) in a microplate. The developed color was read at 410 nm.

### 2.12. Immunofluorescence microscopy

The immunolocalization was performed according to Peroni et al. (2008), with modifications. The starch granules at different stages of ripening were blocked with phosphate buffered saline (PBS), pH 7.2, and 3% BSA (w/v) for 2 h at room temperature, were subsequently incubated with antibodies against banana  $\alpha$ -amylase or  $\beta$ -amylase, and diluted (1:10) in PBS and 3% BSA (w/v) overnight at 4 °C. Then, the starch granules were washed three times with PBS/BSA for 30 min each and incubated for 4 h at room temperature with a secondary antibody, Alexa Fluor 488 goat anti-rabbit IgG (H + L, A-11008, Invitrogen, 2 mg/mL), diluted 1:50. The starch granules were washed again with PBS at pH 7.2. The labeled grains were viewed using a confocal laser scanning microscope (CLMS, Zeiss, Germany, LSM 510), and the images were analyzed in a LSMS Image Browser. The labeled starch granules were quantified using ImageJ 1.46r Program (Wayne Rasband National Institutes of Health, USA). Similarly, the slices (0.5 cm  $\times$  0.5 cm) from frozen bananas pulps (the control fruits at the intermediate stages of ripening) were embedded in O.C.T. (optimal cutting temperature, tissue, Tek 4583) in a cryostat microtome and cut in sections that were 12  $\mu$ m thick. The sections were transferred to glass slides and washed 3 times with phosphate buffered saline (PBS), pH 7.2, and 3% BSA (w/v),

followed by incubation for 2 h with the same buffer as previously described for the starch granules. After incubation with the antibodies and the successive washes, the sections were covered with N-propylgalato (Sigma) and analyzed using a Confocal Laser Scanning Microscope (CLSM, Zeiss, Jena, Turingia, Germany, LSM 510) and the images were analyzed in a laser scanning microscopes (LSM) image browser program.

### 2.13. Pro-Q diamond staining

The analyses were performed according to Glaring et al. (2006). The starch granules at different stages of ripening (50 mg) were incubated with 200  $\mu$ L of 50 mM Tris–HCl (pH 7.5), 10 mM CaCl<sub>2</sub>, and 1 mg/mL of Trypsin and Proteinase K for 4 h at 37 °C. The starches were washed twice with SDS buffer (0.1% SDS, 5 mM EDTA, 50 mM Tris–HCl, pH 8.0) and three times with distilled water. Then, 500  $\mu$ L of the Pro-Q Diamond phosphoprotein gel stain (Molecular Probes) was mixed with the starch granules and incubated at room temperature for 1 h. After washing three times with distilled water, the granules were suspended in 20  $\mu$ L of 50% glycerol. An aliquot of 5  $\mu$ L was mixed with 5  $\mu$ L of 80% glycerol on a glass slide. The SYPRO Ruby (Molecular Probes) staining was performed concomitantly using a similar approach. The labeled grains were viewed using a Confocal Laser Scanning Microscope (CLSM, Zeiss, Jena, Turingia, Germany, LSM 510) and the images were analyzed in a Laser Scanning Microscopes (LSM) Image Browser Program. The labeled starch granules were quantified using ImageJ 1.46r Program (Wayne Rasband National Institutes of Health, USA).

## 3. Results and discussion

### 3.1. Starch granule degradation and morphology

According to Fig. 1, the bananas that were stored at 13 °C (cold-stored group) for 15 days could achieve full ripening after the temperature was increased to 19 °C. However, in comparison to the control bananas, those stored at 13 °C showed not only a delay in starch degradation, but a higher amount (8%) of residual starch, which in turn resulted in approximately half of the amount of soluble sugars in the pulp of the full ripe fruit. This result was a clear indication that the temperature impaired the metabolism of starch; thus, the starch granules obtained from bananas at different ripening stages (referred to as green, intermediate and full ripe bananas in Fig. 1A) were investigated.

The native granules presented birefringence or a Maltese cross when observed by Light microscopy with polarized light (Fig. 2, left column), indicating a radial alignment of the crystalline structure within the starch granule (Pérez & Bertoft, 2010) that persisted even at the advanced ripening stage. When imaged by laser differential interference contrast micrographs (Fig. 2, middle column), the granules isolated from the green bananas of the control group were oval in shape and elongated, with irregular shape and size, and showed smooth surfaces when imaged by SEM (Fig. 2, right column). The degradation caused by enzymatic surface erosion during banana ripening resulted in smaller granules with elongated shape and parallel striations, corresponding to the growth rings exposed by the exo-corrosion process on the starch granule surface as previously reported (Peroni-Okita et al., 2010). In contrast, the granules isolated from the bananas stored at low temperature for 10 days, which were still green, presented pits on the surface with high frequency. These granules preserved the rounded shape, but the striations were rarely observed; the pits, in contrast, were enlarged by the corrosion process, suggesting that the partial degradation occurring at 13 °C was not according to the same mechanism as the degradation that occurs during ripening at 19 °C (Fig. 2). It

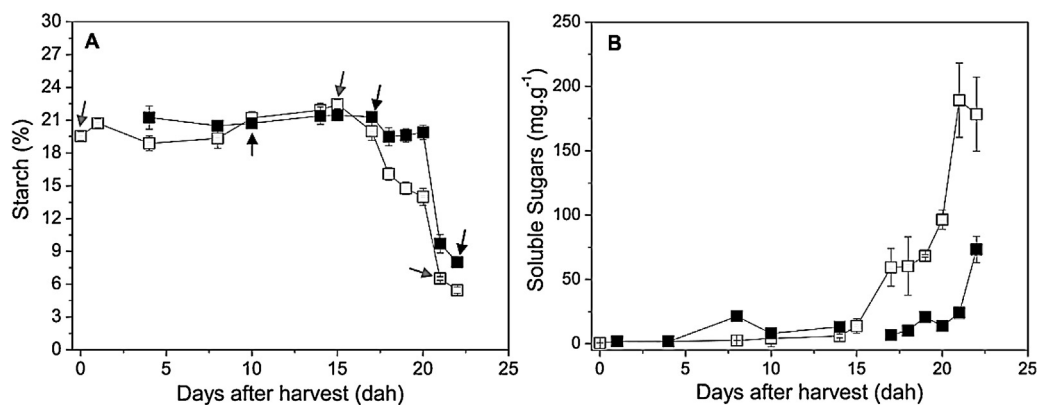


**Fig. 1.** Starch degradation (A) and soluble sugars synthesis (B) during the ripening of Nanicão bananas stored at 19 °C (control fruits, □) and stored at 13 °C (■-). The points represent the mean ( $n=3$ ), and the bars represent the standard deviations. The arrows indicate the stages where starches were isolated from the pulp.

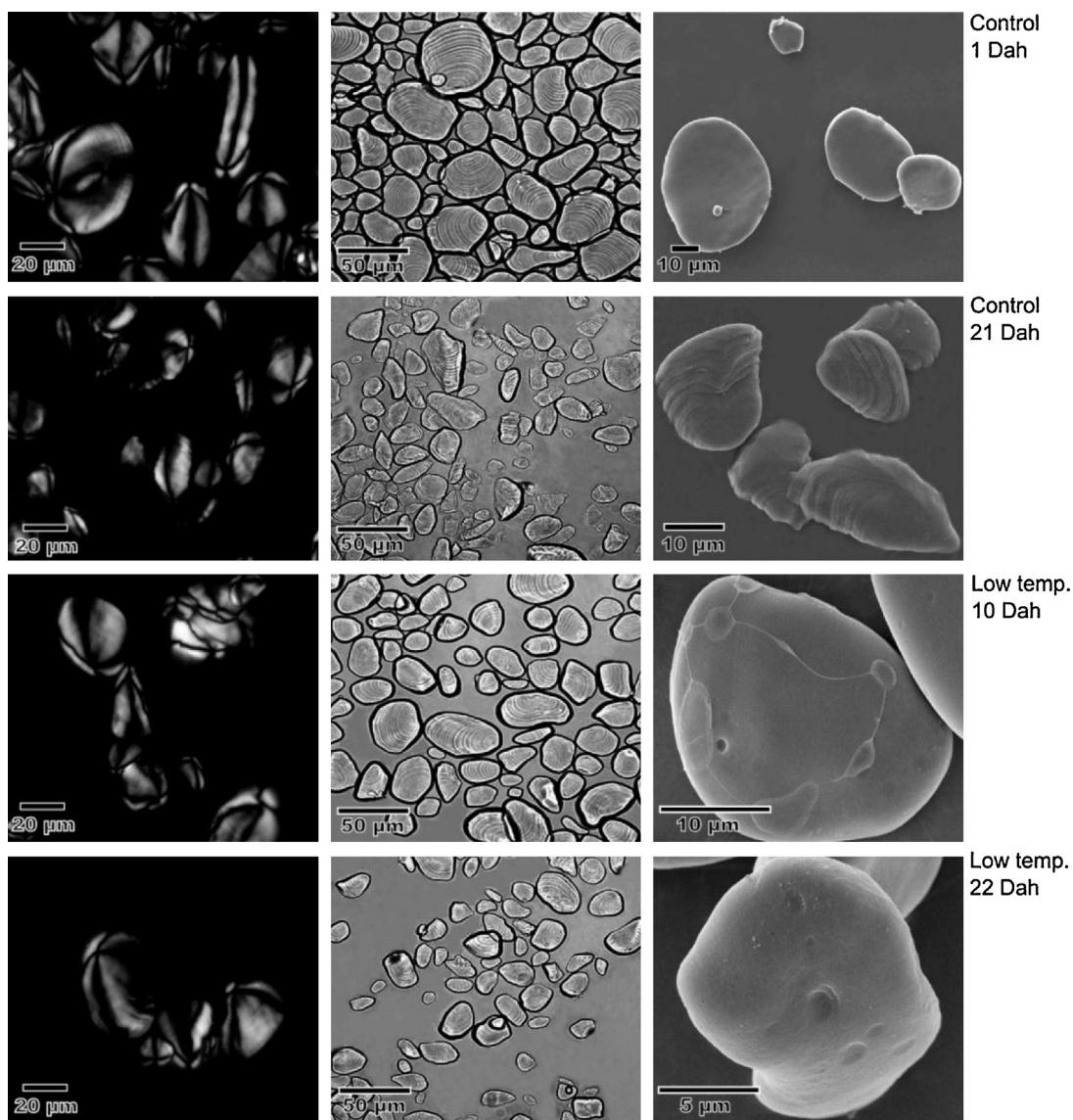


**Fig. 2.** Polarized light optical micrographs (left column), laser differential interference contrast micrographs (middle column), and SEM images (right column) of the starch granules extracted from Nanicão bananas.



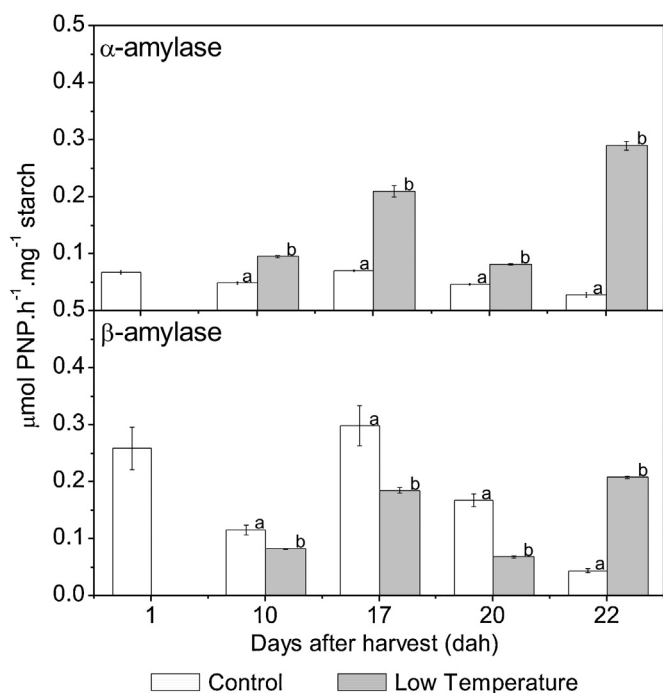


**Fig. 3.** Activities profiles of the  $\alpha$ - and  $\beta$ -amylases associated with the starch granules isolated from Nanicão bananas at different stages of ripening, in control fruits ( $19^{\circ}\text{C}$ ) and cold-stored fruits ( $13^{\circ}\text{C}$ ). The columns represent the mean ( $n=3$ ), and the bars represent the standard deviations. Different letters in the same bars group are significantly different ( $P < 0.05$ ).

is possible this would be a non-complete degradation of the external layer, which would account for the constant synthesis of low amounts of soluble sugars during the cold storage.

## 3.2. Amylases and banana starch degradation

### 3.2.1. Soluble amylases

All of the mentioned differences regarding the appearance of the granules and the amount of carbohydrates point to an effect of the cold storage on the enzymatic pathways of starch degradation. In fact, in cold-stored fruits, the soluble  $\alpha$ -amylase activity was almost the double whereas the soluble  $\beta$ -amylase activity was almost suppressed (Agopian et al., 2011). The enlarged pits on the surface of the granules from the cold-stored fruit (Fig. 2) is reflective of the high  $\alpha$ -amylase activity, and the absence of the striations could be explained by the low  $\beta$ -amylase activity. In fact, the pits are observed in the initial steps of ripening of both the control and cold-stored fruits, but with the advance of ripening, they are not observed in granules from the control samples. This is most likely because a complex of enzymes are acting simultaneously, resulting in the complete degradation of each layer. Because the enzymes are adhered to the surface of the starch granule in the freshly harvested samples (day zero), when there is no detectable starch degradation, it is likely that the initiation of starch degradation would be a response to an unknown signal occurring between days 15 and 20 after harvest. What this signal is remains to be established.

### 3.2.2. Starch granule associated amylases

To confirm the association between the appearance of the starch granule and the degradative enzymes, the activities of the amylases bound to the starch granule surface were evaluated. As observed for the soluble activities, the granule-bound  $\alpha$ -amylase in the cold-stored bananas (Fig. 3) was much higher than those from the control group, whereas the activity of the  $\beta$ -amylase bound to the granules

was much lower. It is already known that  $\alpha$ -amylase can start the degradation process, but the complete degradation of the layers of the granule depends on  $\beta$ -amylase and the debranching enzymes. Therefore, the prevalence of the  $\alpha$ -amylase activity resulted in a high number of pits on the surface of the granules from cold-stored green fruits that were enlarged as the ripening progressed, as observed by SEM (Fig. 2).

### 3.2.3. Immunolocalization of the amylases on the granule surface

The binding of the  $\alpha$ - and  $\beta$ -amylases to the granules surface was confirmed by the immunofluorescence microscopy of starch granules using an antiserum against banana  $\alpha$ - and  $\beta$ -amylases (Fig. 4). When the starch granules isolated from the cold-stored fruits were probed with the  $\alpha$ -amylase antiserum, the immunofluorescence signal was higher than that of the granules from the control group, especially at day 17, in agreement with the enzyme activity assay (Fig. 3). Similarly, starch granules from the cold-stored fruits at day 10 and 17 were more strongly labeled when probed with the  $\beta$ -amylase antiserum than the control group. To confirm these differences among the samples, we quantified the labeled starch granules in Fig. 4 and the results are presented in Fig. SD-1 (Supplementary data).

Because soluble proteins can bind to the starch granule artificially during tissue homogenization, the immunocytochemistry of the intact tissue was employed to confirm the natural occurrence of the amylases bound to the starch granules. The *in situ* localization of the  $\alpha$ - and  $\beta$ -amylase in slices of the banana fruit pulp (Fig. 5) confirmed that the enzymes at the surface of several starch granules localized into the amyloplasts of the banana pulp cells in the fruits of the control group at the intermediate stage of ripening.

The amount of the  $\beta$ -amylase protein and activity appear to depend on the climacteric ethylene, as revealed by the treatment with the ethylene antagonist 1-MCP (Mainardi et al., 2006; Nascimento et al., 2006). In this case, the metabolic pathway of starch degradation through the  $\alpha$ -amylase and phosphorylases steps seems to be prevalent. Based on the previous results by Agopian et al. (2011) and the present work, it seems likely that low temperatures impaired the full induction of  $\beta$ -amylase by ethylene. These findings suggest that another enzymatic pathway can operate to carry out the starch degradation during the ripening of fruits that were previously stored at low temperature ( $13^{\circ}\text{C}$ ).

However, it was noteworthy that both the  $\alpha$ - and  $\beta$ -amylases were already associated with the starch granules isolated from green bananas, even without the typical signs of degradation, i.e., the appearance of striations. It is already known that  $\alpha$ -amylase can initiate the starch degradation process and that  $\beta$ -amylase and isoamylases can act on the granule without  $\alpha$ -amylase activity if the glucosyl units of the amylopectin chain were phosphorylated at the C-6 or C-3 positions. The result indicates that  $\beta$ -amylase had the ability to bind to the starch granule but not to act on the linear and branched glucans released from starch by  $\alpha$ -amylase. The phosphorylation of the starch granule is mediated by the enzymes alpha-glucan, water dikinase (GWD) and phosphoglucan, water dikinase (PWD), respectively (Glaring et al., 2006; Kötting, Kossmann, Zeeman, & Lloyd, 2010; Pérez & Bertoft, 2010; Reimann, Ziegler, & Appenroth, 2007; Zeeman, Kossmann, & Smith, 2010), and the level of phosphorylation varies according to the source, with tuberous starches containing higher amounts than cereal starches (Glaring et al., 2006; Peroni, Rocha, & Franco, 2006). Because the phosphate distribution pattern in the starch granules might be different between the fruit from the two groups under study, the isolated granules were stained with Pro-Q Diamond, a

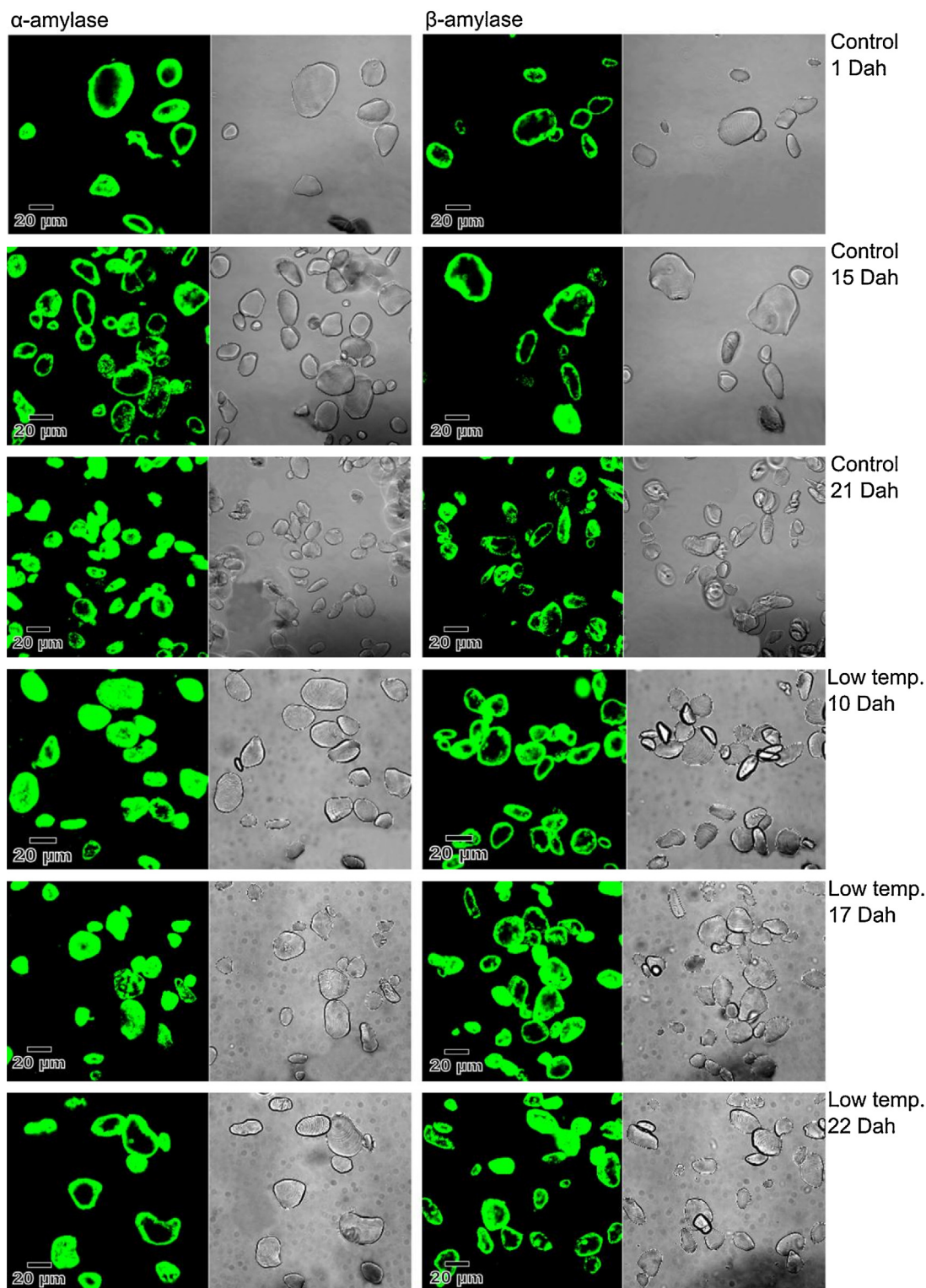


**Fig. 4.** CLSM immunofluorescence images on the starch granules surface isolated from Nanicão bananas using primary antibodies against banana  $\alpha$ -amylase and  $\beta$ -amylase. The secondary antibody Alexa Fluor 488 goat anti-rabbit IgG (H+L) was used.

specific probe to recognize phosphate groups in native starch granules (Glaring et al., 2006).

### 3.3. Phosphorylation of the starch granule

The results (Fig. 6, left column) revealed that the starches isolated from cold-stored bananas presented stronger phosphate staining when compared with control group, even at

the onset of the starch degradation process (days 15 and 17 for the control and cold-stored groups, respectively). However, a small decrease in phosphate staining was observed at the late stages of ripening, for the both groups, suggesting that the granules retained a significant degree of phosphorylation. The intensity of the labeled starch granules was quantified and the results are presented in Fig. SD-2 (Supplementary data).

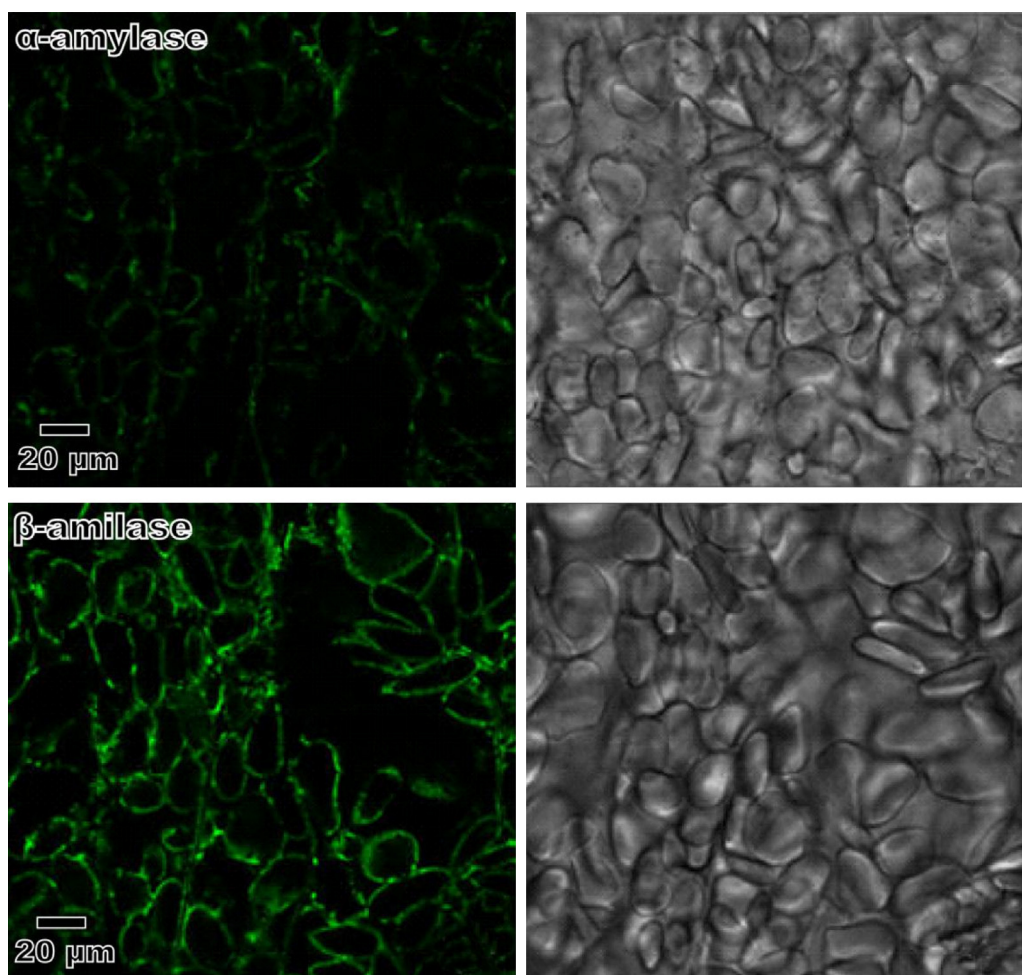


**Fig. 5.** CLSM immunofluorescence images (left column) and transmitted images (right column) on slices of frozen Nanicaõ bananas (control fruits, at intermediate stage of ripening), using the primary antibodies against banana  $\alpha$ -amylase and  $\beta$ -amilase. The secondary antibody Alexa Fluor 488 goat anti-rabbit IgG (H+L) was used.

These results showed that the starches granules were already phosphorylated even at the green stage in freshly harvested bananas, and denote GWD and PWD as part of the ripening apparatus. Thus, phosphorylation did not appear to be a limiting condition for starch degradation in granules from the fruit stored at 13 °C.

The overall results indicate that  $\alpha$ -amylase is not able to operate a complete radial degradation of the starch granules in the cold-stored group, and the optimal action of  $\beta$ -amylase could explain the phosphorylated regions that are still observed at the late stages of ripening (Fig. 6, left and right columns). Apparently, both  $\alpha$ -amylase and  $\beta$ -amylase are able to initiate the degradation of the banana starch granules, and the inhibition of  $\beta$ -amylase by the low temperature may steer the degradation primarily through the  $\alpha$ -amylase pathway, although the degradation of starch was not complete.

#### 3.4. Structural characteristics of starch granules

Because the differences in starch mobilization between the two groups could be dependent not only on the enzymes but also on the structural features of the granules, we determined the amylose content into the starch granules and the amylopectin branch-chain length distribution profile and their relationship with the crystallinity index and the amount of structural water, as well as the general molecular distribution and location of amylose and amylopectin within the granules.

##### 3.4.1. Amylose content

According to Peroni-Okita et al. (2010), the apparent increase in the amounts of amylose in starches isolated from ripening bananas points toward the preferential degradation of regions rich in amylopectin, which results in granules with increasing amounts of amylose. The amylose content ranged from 15.1 to 17.2% for starch isolated from the control bananas during ripening, and starches of cold-stored bananas presented 19.4% of the amylose in the green stage (with 10 days after harvest) and 17.0% at the ripe stage (with 22 days after harvest) (Table 1). Considering the amount of amylose in the ripe bananas of the control and the low temperature groups, the degradation pathway appears to be similar once the fruits were removed from the cold storage. The results allow us to conclude that the central region of the granule is richer in amylose, but no significant differences were observed between the groups.

##### 3.4.2. Amylose localization on the starch granule

The growth rings and the general molecular distribution of amylose and amylopectin in the starch granules were visualized by staining the starch granules with the fluorophore APTS, followed by analysis by CLSM (Fig. 7). The CLSM sections showed clear brightly stained growth rings around the fluorescent hilum and in the direction of the surface of the granules. It has previously been shown that the amylose appears to be interspersed among the amylopectin molecules, being located primarily in the amorphous regions of the granule (Glaring et al., 2006; Jane, 2006; Pérez & Bertoft, 2010). Although some reports have suggested that amylose



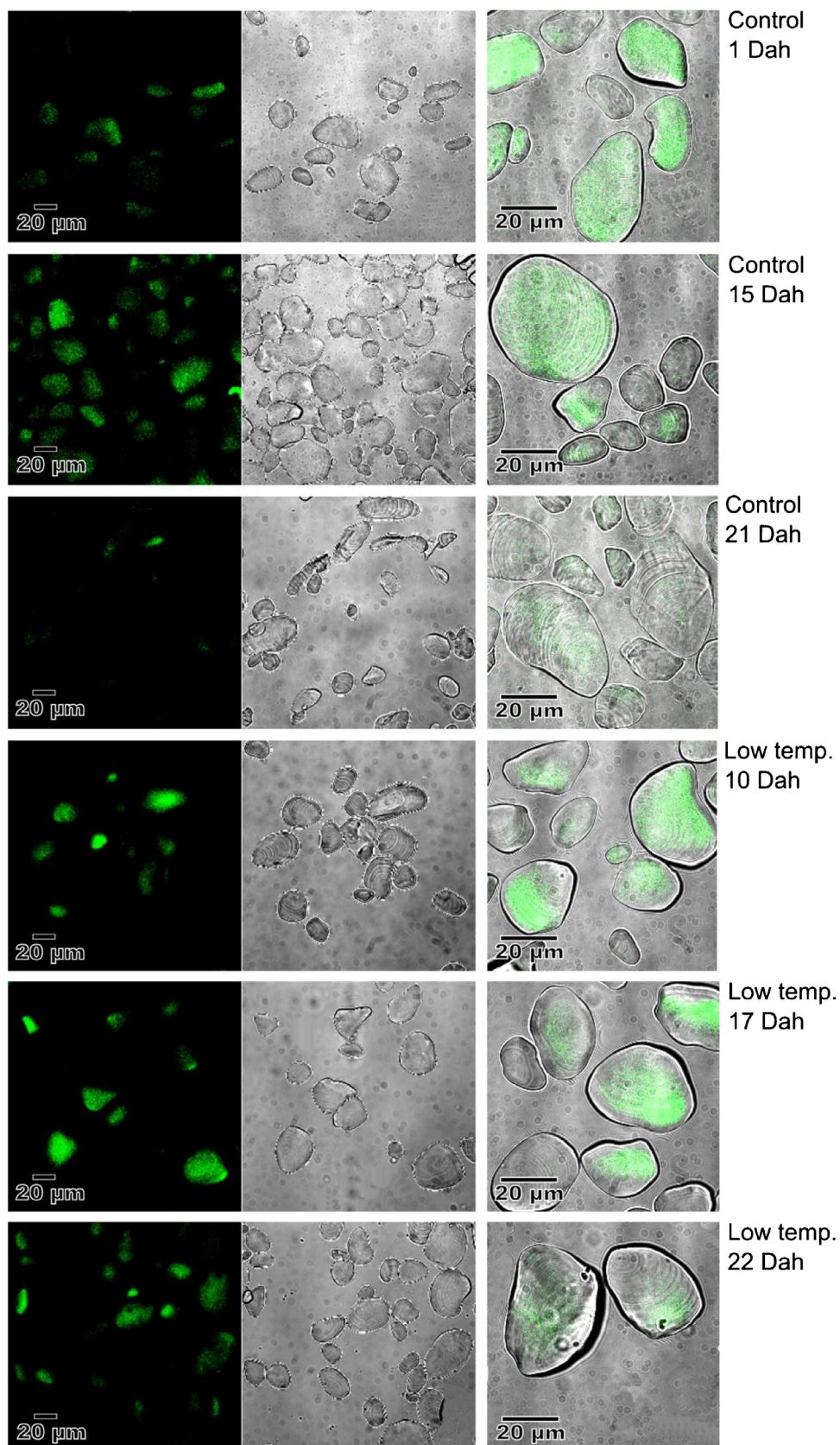


**Fig. 6.** CLSM immunofluorescence images (left column) of the starch granules isolated from Nanicão bananas stained with Pro-Q and transmitted images (middle column). The right column contains immunofluorescence and transmitted superposed images.



**Table 1**  
Amylose content, branch-chain length distributions, crystallinity degree and relaxation times ( $T_2H$ ) of starch granules isolated from Nanicão bananas.

Starch	Days after harvest	Amylose content <sup>a</sup> (%)	Chain length distribution <sup>b</sup>				fa/fb <sub>1</sub> + fb <sub>2</sub> + fb <sub>3</sub>	Crystallinity degree <sup>a</sup> (%)	A-type content <sup>a</sup> (%)	B-type content <sup>a</sup> (%)	$T_2H$ (ms) 27 °C	$T_2H$ (ms) 50 °C
			fa	fb <sub>1</sub>	fb <sub>2</sub>	fb <sub>3</sub>						
Control	1	15.1 ± 0.2	26	57	13	4	0.35	23.8 ± 2.2	53 ± 2	47 ± 2	0.7	0.8
	21	17.2 ± 0.9	25	56	13	5	0.33	25.4 ± 2.8	50 ± 3	50 ± 3	0.6	48.8
Low temperature	10	19.4 ± 2.3	31	53	11	4	0.45	26.8 ± 2.4	55 ± 2	45 ± 2	0.7	53.8
	22	17.0 ± 2.5	24	57	14	5	0.32	25.0 ± 2.3	56 ± 2	44 ± 2	0.8	54.7

<sup>a</sup> Mean values at least three replicates per sample.

<sup>b</sup> Sum of peak-area ratios (%) of group with degree of polymerization (dp). Fractionation was as follows: fa, dp 6–12; fb<sub>1</sub>, dp 13–24; fb<sub>2</sub>, 25–36; fb<sub>3</sub>, ≥37.

is more concentrated near the granule surface, the results revealed that amylose was concentrated in the amorphous regions between the growth rings and in the central region around the hilum. In addition, the CLSM images reinforce the idea that the formats of starch granules from ripe bananas from the cold-stored group are different than those from the control group.

#### 3.4.3. Amylopectin branch-chain length distributions

The amylopectin branch-chain length distributions give an idea of the composition of the chains inside the starch granule. The chains can be divided into fractions *fa*, *fb*<sub>1</sub>, *fb*<sub>2</sub> and *fb*<sub>3</sub> (Hanashiro, Abe, & Hizukuri, 1996). The amylopectin from the green bananas stored at 13 °C for 10 days had a large amount of the short *fa*-chain (dp 6–12, 31%, Table 1), which is correlated with the type of crystallinity of the granules (Pérez & Bertoft, 2010). Among the others fractions, *fb*<sub>1</sub>-chain (dp 13–24) was the most abundant in all of the starches, as observed by Hanashiro et al. (1996), and Peroni-Okita et al. (2010), while the long amylopectin *fb*<sub>3</sub>-chains (dp ≥ 37) presented the lowest amount.

The starches obtained from the fruit cold-stored for 10 days not only had a larger amount of short *fa*-chains but also had lower values for the other fractions (*fb*<sub>1</sub> and *fb*<sub>2</sub>, Table 1). It is likely these *fb*<sub>1</sub> and *fb*<sub>2</sub>-chains were preferentially degraded during cold storage and could account for the sugar synthesis that occurred under this condition. After the fruits were removed from cold storage to ripen at a higher temperature, the degradation of all of the chains appeared to be similar to the control group.

According to Hanashiro et al. (1996), and Peroni-Okita et al. (2010), the ratio  $fa/(fb_1 + fb_2 + fb_3)$  can be used to estimate the branch-chain length of amylopectin. Larger ratios reveal the degree of amylopectin ramification. The starch from the mature fruits, from both the control and cold-stored groups, presented the lowest values (0.33 and 0.32, respectively). The larger ratio (0.45) for the cold-stored fruits at 10 days indicate a higher degree of ramification of amylopectin and a larger proportion of short chains, resulting from the incomplete starch degradation.

There is a positive correlation between the degree of crystallinity and the proportion of amylopectin (Peroni-Okita et al., 2010), and the amount of the *fa* fraction plays an important role in determining the polymorphic forms of starch crystals.

#### 3.4.4. Crystallinity index

Wide-angle X-ray diffraction (WAXD) was used to observe the crystalline structure and polymorphism of the starch granules that exhibited the C-type crystalline structure for all samples. Table 1 shows the crystallinity index as well as the A- and B-type content for each starch. The starches isolated from the control fruits with 1 and 21 days after harvest presented similar crystallinity index (23.8 ± 2.2 and 25.4 ± 2.8%, respectively). The proportions of the A- and B-type allomorphs in the green fruits were 53 ± 2 and 47 ± 2%, respectively, and were 50 ± 3% for each allomorph in the mature stage. Although the cold-stored fruits were also similar within the error bars, subtle differences were observed, with a reduction in the crystallinity index from 26.8 ± 2.4% to 25.0 ± 2.3% as a consequence

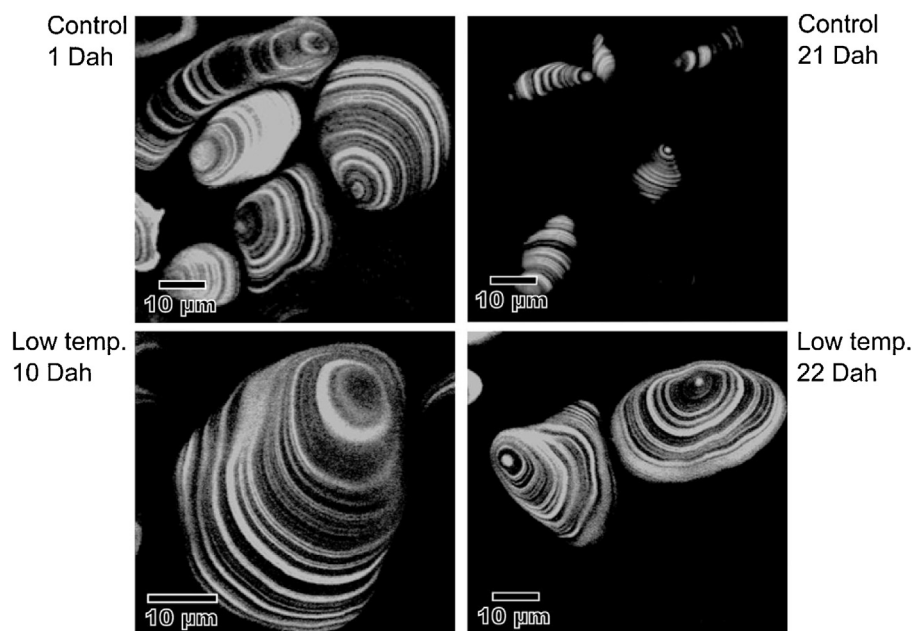


**Fig. 7.** CLSM optical sections of the starch granules isolated from Nanicão bananas stained with the fluorophore APTS.

of banana ripening. The A-type content increased slightly from  $55 \pm 2$  to  $56 \pm 2\%$ , while the B-type decreased from  $45 \pm 2$  to  $44 \pm 2\%$ . As found by Peroni-Okita et al. (2010), the A-type crystallites are located on the periphery of the starch granules in the control fruits and are preferentially degraded because no degradation of the B-type allomorph (Table 1) was found inside of the granule during the ripening process. In general, it appears that there was a subtle degradation of the short *fa*-chains and of the A-type allomorph (Table 1) during banana ripening, although no reduction in the crystallinity index was observed in the control fruits.

#### 3.4.5. Molecular mobility

Molecular mobility is another property of the organization of the polymer chains in native starch granules studied by relaxation experiments (Kulik & Haverkamp, 1997) because the water distribution is known to be an integral part of the crystalline unit within the starch granules (Perry & Donald, 2000). Moreover, NMR studies provide information about the interactions that occur in the sample and allow us to evaluate the plasticization effect (Maciel & Tavares, 2010). Table 1 shows the proton spin-spin relaxation time values,  $T_2H$ , for all of the starches. The analysis at  $27^\circ\text{C}$  did not show differences during starch degradation and between the control and cold-stored fruits. However, for the starches analyzed at  $50^\circ\text{C}$ , the  $T_2H$  increased from 0.8 to 48.8 ms for the control fruits during starch degradation whereas the starches from the cold-stored fruits showed similar values over the ripening of the fruits (53.8 and 54.7 ms). The lower value found in the green control starch with 1 day after harvest suggests that the granule surface is covered by a harder or inelastic material that is uniformly distributed on its surface, as suggested previously by Peroni-Okita et al. (2010) for banana starch granules analyzed by AFM technique. When the ripening of fruits is fully completed, the  $T_2H$  increased to 48.8 ms, suggesting an increase of water mobility due to the plasticizing effects. This event occurs concomitantly with the enzymatic attack on the granule surface, which removed the initial layer and allowed the new layer to be visualized. The new layer formed was likely composed by both hard and soft regions, as visualized by AFM (Peroni-Okita et al., 2010), with different viscoelastic properties. However, the presence of only one domain for all of the starches (Table 1) suggests that banana starch presents a homogeneous structural behavior according to their molecular organization, inter- and intramolecular interactions and water distribution within the starch granules. Nevertheless, as reported by Choi and Kerr (2003), some starches present multiple relaxation times, indicating that more than one population of water existed in the starch; this has been interpreted as the water mobility or “bound” water.

## 4. Conclusion

Based on the activities of the enzymes, it is appears that a low temperature favored the starch degradation through the  $\alpha$ -amylase pathway over that of the  $\beta$ -amylase pathway in cold-stored bananas, which resulted in different structural features of the starch granules. The low temperature led to a predominance of rounded granules and pits on the surface, along with a higher amylose content during cold storage. These results, combined with the abundance of short *fa*-chains of amylopectin, suggest that the *fb*<sub>1</sub> and *fb*<sub>2</sub>-chains were preferentially degraded during the 10 days of storage at low temperature. The higher amounts of *fa*-chains probably contributed to the higher values of the A-type content and crystallinity degree. Additionally, the increased molecular mobility would facilitate the intake of  $\alpha$ -amylase and its action on the granule surface, where it was the prevalent enzyme. It appears that the final quality of the fruit was negatively affected by the lower

percentage of starch degradation and synthesis of soluble sugars resulting from the decreased action of  $\beta$ -amylase.

## Acknowledgments

NLNS is acknowledged through the project MX1-6948 (XRD). The authors acknowledge the Fundação de Amparo à Pesquisa do Estado de São Paulo (FAPESP) and Conselho Nacional de Desenvolvimento Científico e Tecnológico (CNPq) for financial support and for the scholarship. The authors acknowledge the BRASNICA and MAGÁRIO Companies for the banana samples.

## Appendix A. Supplementary data

Supplementary data associated with this article can be found, in the online version, at <http://dx.doi.org/10.1016/j.carbpol.2013.03.050>.

## References

- Agopian, R. G., Peroni-Okita, F. H. G., Soares, C. A., Mainardi, J. A., Nascimento, J. R. O., Cordenunsi, B. R., et al. (2011). Low temperature induced changes in activity and protein levels of the enzymes associated to conversion of starch to sucrose in banana fruit. *Postharvest Biology and Technology*, *62*, 133–140.
- Blennow, A., Hansen, M., Schulz, A., Jorgensen, K., Donald, A. M., & Sanderson, J. (2003). The molecular deposition of transgenically modified starch in the starch granule as imaged by functional microscopy. *Journal of Structural Biology*, *143*, 229–241.
- Cardoso, M. B., & Westfahl, H., Jr. (2010). On the lamellar width distributions of starch. *Carbohydrate Polymers*, *81*, 21–28.
- Chauhan, O. P., Rajei, P. S., Dargupta, D. K., & Bawa, A. S. (2006). Instrumental texture changes in banana during ripening under active and passive modified atmosphere. *International Journal of Food Properties*, *9*, 237–253.
- Choi, S. G., & Kerr, W. L. (2003).  $^1\text{H}$  NMR studies of molecular mobility in wheat starch. *Food Research International*, *36*, 341–348.
- Glaring, M. A., Koch, C. B., & Blennow, A. (2006). Genotype-specific spatial distribution of starch molecules in the starch granule: A combined CLMS and SEM approach. *Biomacromolecules*, *7*, 2310–2320.
- Hanashiro, I., Abe, J. I., & Hizukuri, S. (1996). A periodic distribution of the chain length of amylopectin as revealed by high-performance anion-exchange chromatography. *Carbohydrate Research*, *283*, 151–159.
- Imahori, Y., Takemura, M., & Bai, J. (2008). Chilling-induced oxidative stress and antioxidant responses in mume (*Prunus mume*) fruit during low temperature storage. *Postharvest Biology and Technology*, *49*, 54–60.
- Jane, J.-L. (2006). Current understanding on starch granule structures. *Journal of Applied Glycoscience*, *53*, 205–213.
- Kötting, O., Kossmann, J., Zeeman, S. C., & Lloyd, J. R. (2010). Regulation of starch metabolism: The age of enlightenment? *Current Opinion in Plant Biology*, *13*, 321–329.
- Kulik, A. S., & Haverkamp, J. (1997). Molecular mobility of polysaccharide chains in starch investigated by two-dimensional solid-state NMR spectroscopy. *Carbohydrate Polymers*, *34*, 49–54.
- Lichtemberg, L. A., Malburg, J. L., & Hinz, R. H. (2001). Susceptibilidade varietal de frutos de bananeira ao frio. *Revista Brasileira de Fruticultura*, *23*, 568–572.
- Maciel, P. M. C., & Tavares, M. I. B. (2010). Solid state and proton relaxation NMR study of dipteryx alata vogel. *Journal of Applied Polymer Science*, *116*, 50–54.
- Mainardi, J. A., Purgatto, E., Vieira-Junior, A., Bastos, W. A., Cordenunsi, B. R., Nascimento, J. R. O., et al. (2006). Effects of ethylene and 1-methylcyclopropene (1-MCP) on gene expression and activity profile of  $\alpha$ -1,4 glucan-phosphorylase during banana ripening. *Journal of Agricultural and Food Chemistry*, *54*, 7294–7299.
- Martínez-Romero, D., Serrano, M., & Valero, D. (2003). Physiological changes in pepino (*Solanum muricatum* Ait.) fruit stored at chilling and non-chilling temperatures. *Postharvest Biology and Technology*, *30*, 177–186.
- Nascimento, J. R. O., Vieira-Junior, A., Bassinello, P. Z., Cordenunsi, B. R., Mainardi, J. A., Purgatto, E., et al. (2006). Beta-amylase expression of starch degradation during banana ripening. *Postharvest Biology and Technology*, *40*, 41–47.
- Pérez, S., & Bertoft, E. (2010). The molecular structures of starch components and their contribution to the architecture of starch granules: A comprehensive review. *Starch/Stärke*, *62*, 389–420.
- Peroni, F. H. G., Rocha, T. S., & Franco, C. M. L. (2006). Some structural and physico-chemical characteristics of tuber and root starches. *Food Science and Technology International*, *12*, 505–513.
- Peroni, F. H. G., Koike, C., Louro, R. P., Purgatto, E., Nascimento, J. R. O., Lajolo, F. M., et al. (2008). Mango starch degradation. II. The binding of alpha-amylase and beta-amylase to the starch granule. *Journal of Agricultural and Food Chemistry*, *56*, 7416–7421.

- Peroni-Okita, F. H. G., Simão, R. A., Cardoso, M. B., Soares, C. A., Lajolo, F. M., & Cordenunsi, B. R. (2010). In vivo degradation of banana starch: Structural characterization of the degradation process. *Carbohydrate Polymers*, *81*, 291–299.
- Perry, P. A., & Donald, A. M. (2000). SANS study of the distribution of water within starch granules. *International Journal of Biological Macromolecules*, *28*, 31–39.
- Reimann, R., Ziegler, P., & Appenroth, K. J. (2007). The binding of  $\alpha$ -amylase to starch plays a decisive role in the initiation of storage starch degradation in turions of *Spirodela polyrrhiza*. *Physiologia Plantarum*, *129*, 334–341.
- Seymour, G. B., Taylor, J. E., & Tucker, G. A. (1993). *Biochemistry of fruit ripening* (1st ed.). London: Chapman & Hall.
- Soares, C. A., Peroni-Okita, F. H. G., Cardoso, M. B., Shitakubo, R., Lajolo, F. M., & Cordenunsi, B. R. (2011). Plantain and banana starches: Granule structural characteristics explain the differences in their starch degradation patterns. *Journal of Agricultural and Food Chemistry*, *59*, 6672–6681.
- Thys, R. C. S., Westfahl, H., Jr., Noreña, C. P. Z., Marczak, L. D. F., Silveira, N. P., & Cardoso, M. B. (2008). Effect of the alkaline treatment on the ultrastructure of C-type starch granules. *Biomacromolecules*, *9*, 1894–1901.
- Wills, R., McGlasson, B., Graham, D., & Joyce, D. C. (1998). *Postharvest: An introduction to the physiology and handling of fruit, vegetables and ornamentals* (4th ed.). Wallingford: New South Wales University Press.
- Zamorano, J. P., Dopico, B., Lowe, A. L., Wilson, I. D., Grierson, D., & Merodio, C. (1994). Effect of low temperature storage and ethylene removal on ripening and gene expression changes in avocado fruit. *Postharvest Biology and Technology*, *4*, 331–342.
- Zeeman, S. C., Kossmann, J., & Smith, A. M. (2010). Starch: Its metabolism, evolution, and biotechnological modification in plants. *Annual Review of Plant Biology*, *61*, 209–234.